JOURNAL OF GEOPHYSICAL RESEARCH, VOL. 114, D23302, doi:10.1029/2008JD010946, 2009

Estimating the contribution of strong daily export events to total pollutant export from the United States in summer

Yuanyuan Fang,[1,2] Arlene M. Fiore,[2] Larry W. Horowitz,[1,2] Anand Gnanadesikan,[1,2] Hiram Levy II,[2] Yongtao Hu,[3] and Armistead G. Russell[3]

Received 6 August 2008; revised 9 August 2009; accepted 21 August 2009; published 4 December 2009.

[1] While the export of pollutants from the United States exhibits notable variability from day to day and is often considered to be "episodic," the contribution of strong daily export events to total export has not been quantified. We use carbon monoxide (CO) as a tracer of anthropogenic pollutants in the Model of OZone And Related Tracers (MOZART) to estimate this contribution. We first identify the major export pathway from the United States to be through the northeast boundary (24–48°N along 67.5°W and 80–67.5°W along 48°N), and then analyze 15 summers of daily CO export fluxes through this boundary. These daily CO export fluxes have a nearly Gaussian distribution with a mean of 1100 Gg CO day^{-1} and a standard deviation of 490 Gg CO day^{-1}. To focus on the synoptic variability, we define a "synoptic background" export flux equal to the 15 day moving average export flux and classify strong export days according to their fluxes relative to this background. As expected from Gaussian statistics, 16% of summer days are "strong export days," classified as those days when the CO export flux exceeds the synoptic background by one standard deviation or more. Strong export days contributes 25% to the total export, a value determined by the relative standard deviation of the CO flux distribution. Regressing the anomalies of the CO export flux through the northeast U.S. boundary relative to the synoptic background on the daily anomalies in the surface pressure field (also relative to a 15 day running mean) suggests that strong daily export fluxes are correlated with passages of midlatitude cyclones over the Gulf of Saint Lawrence. The associated cyclonic circulation and Warm Conveyor Belts (WCBs) that lift surface pollutants over the northeastern United States have been shown previously to be associated with long-range transport events. Comparison with observations from the 2004 INTEX-NA field campaign confirms that our model captures the observed enhancements in CO outflow and resolves the processes associated with cyclone passages on strong export days. "Moderate export days," defined as days when the CO flux through the northeast boundary exceeds the 15 day running mean by less than one standard deviation, represent an additional 34% of summer days and 40% of total export. These days are also associated with migratory midlatitude cyclones. The remaining 35% of total export occurs on "weak export days" (50% of summer days) when high pressure anomalies occur over the Gulf of Saint Lawrence. Our findings for summer also apply to spring, when the U.S. pollutant export is typically strongest, with similar contributions to total export and associated meteorology on strong, moderate and weak export days. Although cyclone passages are the primary driver for strong daily export events, export during days without cyclone passages also makes a considerable contribution to the total export and thereby to the global pollutant budget.

Citation: Fang, Y., A. M. Fiore, L. W. Horowitz, A. Gnanadesikan, H. Levy II, Y. Hu, and A. G. Russell (2009), Estimating the contribution of strong daily export events to total pollutant export from the United States in summer, *J. Geophys. Res.*, *114*, D23302, doi:10.1029/2008JD010946.

1. Introduction

[2] The United States is a major source of anthropogenic trace gases to the global atmosphere [*Nichols et al.*, 2001]. Transport of pollutants within the midlatitudes, especially export from East Asia and North America, exhibits notable variability in time and thus is often referred to as "episodic"

[1]Atmospheric and Oceanic Sciences Program, Princeton University, Princeton, New Jersey, USA.
[2]Geophysical Fluid Dynamics Laboratory, Princeton, New Jersey, USA.
[3]School of Civil and Environmental Engineering, Georgia Institute of Technology, Atlanta, Georgia, USA.

0148-0227/09/2008JD010946

[e.g., *Cooper et al.*, 2001]. Previous studies show that pollutants from the United States affect European and global air quality both through strong export events and by enhancing the hemispheric pollutant burden [*Stohl and Trickl*, 1999; *Li et al.*, 2002; *Holloway et al.*, 2003; *Auvray and Bey*, 2005; *Huntrieser et al.*, 2005; *Derwent et al.*, 2004; *Guerova et al.*, 2006]. However, there is no consistent definition for "episodic export," confounding attempts to quantify the extent of episodicity and the contribution from episodic export to the total pollutant burden. Here, we apply a global 3-D chemical transport model (MOZART) to develop a statistical definition of strong export days in order to estimate their contribution to total pollutant export from the United States.

[3] Studies of episodic export have usually focused on downwind concentration enhancements in observations [*Stohl and Trickl*, 1999; *Huntrieser et al.*, 2005] or models [*Li et al.*, 2002, 2005; *Auvray and Bey*, 2005]. For example, *Li et al.* [2002] found that North American anthropogenic emissions contribute up to 10–20 ppbv to surface O_3 at Mace Head, Ireland during transatlantic transport events. *Guerova et al.* [2006] showed that during export events emissions from North America can result in O_3 enhancements of up to 25–28 ppb between 800 and 600 hPa and 10–12 ppb in the boundary layer over Europe. Meanwhile, the background hemispheric O_3 burden enhancement due to North American anthropogenic emissions has been shown to contribute an average of 2–4 ppbv to European surface O_3 during summer [*Li et al.*, 2002] and 11% to the total O_3 annual burden over Europe [*Auvray and Bey*, 2005].

[4] While some of these studies [e.g., *Li et al.*, 2002; *Guerova et al.*, 2006] compare the influence of emissions from the North American source region on concentrations in a receptor region (e.g., Europe) by enhancing the hemispheric background versus by direct transport during episodic export events, they have not quantified the contribution from episodic export to the total export. This is partly due to the reliance on concentration-oriented methods, which focus on plumes at specific locations, and therefore cannot be used to estimate the overall contribution of this export on the global pollutant budget. For instance, *Li et al.* [2005] defined North American episodic "outflow events" in July in their model (for the 4 years they simulated) as periods with North American anthropogenic CO mixing ratios greater than 50 ppb at 950 hPa across a plane at 70°W. However, if we apply their metric to estimate the episodic contribution to North American export, such "plumes" persist throughout July in some years, suggesting that "episodic export" contributes nearly 100% to the total export of pollution. Although there is no standard definition of "episodic export," the term "episodic" implies a fluctuating condition and thus this definition of *Li et al.* [2005] is clearly not applicable for our study.

[5] Meteorology is a major driver of the variability in pollutant export from the United States. Previous studies show that the typical export process involves the accumulation of pollutants under a high pressure system, followed by the passage of a migratory midlatitude cyclone that sweeps these pollutants offshore [e.g., *Vukovich*, 1995; *Merrill and Moody*, 1996]. The Warm Conveyor Belts (WCBs) ahead of cold fronts associated with these midlatitude cyclones can lift pollutants to the middle and upper troposphere, and have been identified as the most important pathway for rapid and direct long-range transport [e.g., *Wild et al.*, 1996; *Wild and Akimoto*, 2001; *Stohl and Trickl*, 1999; *Stohl et al.*, 2003; *Cooper et al.*, 2001, 2004; *Trickl et al.*, 2003; *Huntrieser et al.*, 2005]. A westward extension of the Bermuda High and deep convection may also contribute to export events [*Li et al.*, 2005; *Auvray and Bey*, 2005; *Owen et al.*, 2006; *Kiley and Fuelberg*, 2006a].

[6] The NASA Intercontinental Chemical Transport Experiment–North America (INTEX-NA) [*Singh et al.*, 2006] is part of the International Consortium for Atmospheric Research on Transport and Transformation (ICARTT) field campaign over North America during July–August 2004. It presents a valuable opportunity to directly examine the outflow from the United States and to evaluate the capability of our model to represent export processes. During the INTEX-NA campaign, a weak Bermuda High was located over the North Atlantic and frontal passages occurred more frequently than on average between 2000 and 2005 [*Fuelberg et al.*, 2007]. Several studies have already examined the outflow from the United States for this period and identified cases of anthropogenic plumes associated with cyclone passages [*Kiley and Fuelberg*, 2006a; *Kiley and Fuelberg*, 2006b]. Consequently, this time period is expected to be a good test case for studying episodic export driven by meteorology.

[7] We largely focus on summer, when photochemically active pollutants in the continental U.S. boundary layer, i.e., reactive nitrogen (NO_y) and O_3, are highest. We use CO as a tracer of pollutant outflow in a 3D global chemical transport model (MOZART, described in section 2). We then identify the major pathway for U.S. pollutant export and develop a flux-based method to define strong export days through this pathway (section 3). Using observations during the INTEX-NA field campaign, we evaluate our model and investigate the processes contributing to strong export days (section 4). Finally, we estimate the contribution of strong export days to total export, examine the sensitivity of this contribution to assumptions in our approach, analyze the meteorological patterns associated with "strong," "moderate" and "weak" export days and extend our analysis to springtime (section 5). Conclusions and implications of this study are given in section 6.

2. Model

2.1. Model Description

[8] The Model of OZone and Related Tracers (MOZART) version 4 is updated from MOZART-2 [*Horowitz et al.*, 2003] with aerosol chemistry based on that of *Tie et al.* [2005]. Its chemistry module includes an improved representation of nonmethane hydrocarbons and online calculation of aerosols [*Horowitz et al.*, 2007]. Updates to the chemistry in MOZART-4 are described by *Emmons et al.* [2006].

[9] The model resolution is 1.9° latitude by 1.9° longitude, with 64 vertical levels. Meteorological fields are taken from the NCEP Global Forecast System every three hours. Global anthropogenic, biomass burning, and natural emissions are updated from those used by *Horowitz et al.* [2003] based on the POET emission inventory for 1997 (http://www.Aero.jussieu.fr/projet/ACCENT/POET.php [*Olivier et al.*, 2003]). Over North America during the summer, we use

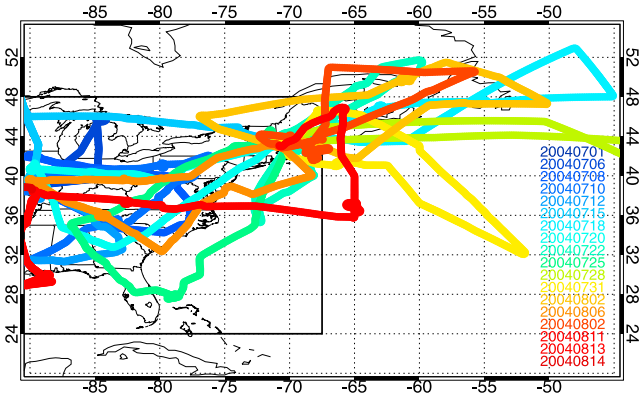

Figure 1. NASA DC-8 flight tracks during the INTEX-NA campaign over eastern North America (July 1 to August 14, 2004). Flight segments used to calculate the regional mean profiles in Figure 2 are contained within the black solid lines.

daily biomass burning emissions developed by *Turquety et al.* [2007] and implemented as described by *Horowitz et al.* [2007]. We use anthropogenic surface emissions for the United States from the EPA National Emission Inventory (NEI99, version 3, http://www.epa.gov/ttn/chief/net/1999inventory.html) except that we update the U.S. anthropogenic NO_x surface emissions for the summer of 2004 to account for the 50% decreases in eastern U.S. NO_x power plant emissions under the State Implementation Plan call between 1999 and 2003 [*Frost et al.*, 2006; *Hudman et al.*, 2007]. We also increase the lightning NO_x source over northern midlatitude continents by a factor of 10 and the fraction emitted into the free troposphere (FT) from 80% to 98%. This change has little influence on CO, but improves the simulation of other species [*Hudman et al.*, 2007; *Ott et al.*, 2007; *Pickering et al.*, 2006; *Fang et al.*, 2008].

[10] Our simulation for the INTEX-NA campaign is conducted from December 2003 through August 2004, with the updated emission inventory for INTEX-NA (NEI99 with 2004 U.S. NO_x emissions) implemented in May 2004, allowing for a two month spin-up to capture changes in the summertime continental boundary layer chemistry. We "tag" two CO tracers in this simulation to track the North American "fossil fuel" (including biofuel) and biomass burning emissions (NAFF CO and NABB CO), following the approach of *Staudt et al.* [2001] and *Bey et al.* [2001]. The "NA" region includes emissions from the United States, Canada and Mexico, with the United States being the largest contributor to anthropogenic CO emissions (around 90%) [*Olivier and Berdowski*, 2001].

[11] To provide an interannual context, we also analyze total daily CO export fluxes from a 15 year simulation (1990–2004) in MOZART-2 [*Fiore et al.*, 2006]. Note that the separate NAFF and NABB CO tracers are not included in this run. This simulation is driven by NCEP reanalysis meteorological fields at 1.9° × 1.9° horizontal resolution with 28 vertical levels. Emissions of all O_3 precursors are held constant from year to year except for lightning NO_x, which changes with meteorology. This simulation enables us to characterize the influence of meteorology on the variability of pollutant export from the U.S. boundary layer.

2.2. Model Evaluation

[12] We evaluate the INTEX-NA simulation by comparing simulated CO with observations made onboard the NASA DC-8 aircraft during the INTEX-NA campaign (July 1 to August 14, 2004, Figure 1) over North America [*Singh et al.*, 2006]. This aircraft typically aimed to sample regionally representative air masses, suitable for comparison with our global model.

[13] Figure 2 shows the mean observed and simulated vertical profiles of CO within the INTEX-NA region. The CO maximum within the boundary layer results from North American surface CO emissions. As the influence from surface emissions weakens, CO concentrations decrease with height up to about 3–4 km. Major sources for CO in the free troposphere include methane oxidation and transport from other regions. CO shows little vertical gradient in the free troposphere, reflecting its 1–2 month lifetime. At 0–2 km above surface, our model overestimates the mean CO mixing ratios by around 20 ppb, likely due to an overestimate of CO anthropogenic emissions [*Hudman et al.*, 2007]. Meanwhile, the model also overestimates the variability of CO mixing ratios within this layer (a standard deviation of 41 ppb from the model versus that of 30 ppb from the observation). However, above 2 km, the simulated mean CO mixing ratio is 9–16 ppb lower than observed and the corresponding simulated variability is also lower than observed, especially at the 2–4 km layer, where the simu-

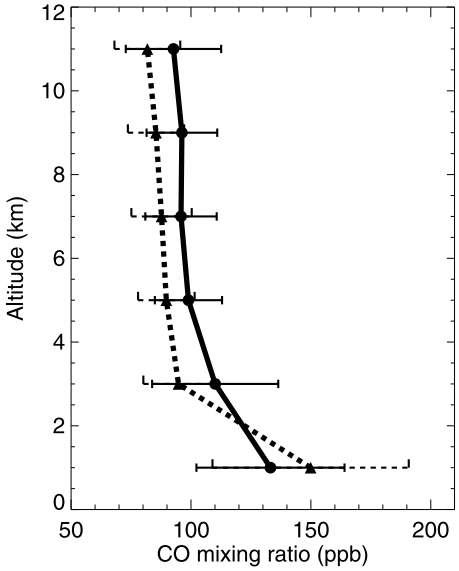

Figure 2. Mean vertical profiles of CO mixing ratios during the INTEX-NA campaign (July 1 to August 14, 2004) from observations on the DC-8 aircraft (solid line) and from the MOZART INTEX-NA simulation (dashed line). Horizontal bars show the standard deviations of each data set within each 2 km layer. Simulated concentrations are sampled every minute along all the flight tracks so as to be comparable with the observations. Both observed and simulated data are averaged within each horizontal model grid box in 2 km altitude bins, and these gridded data are then averaged (area-weighted) within the region shown in Figure 1 to obtain regional mean profiles.

Table 1. Budget of Total CO and NAFF CO From the INTEX-NA Simulation for July 2004[a]

	CO	NAFF CO
Emission	10.1	8.3
Production	11.4	
Loss	−13.3	−2.2
Burden	9.4	1.3
Export		
NE[b]	−28.5	−5.2
Rest of north[c]	4.5	−0.4
South	4.6	∼0

[a]Unit: Tg, positive values indicate net source to this region while negative value indicate net sink to this region.

[b]Export through the northeast boundary, including the east boundary (24–48°N, along 67.5°W) and the eastern part of the north boundary (80–67.5°W, along 48°N).

[c]Export through the western part of the north boundary (127.5–80°W, along 48°N).

lated standard deviation is 15 ppb versus 25 ppb observed. Throughout the troposphere over the eastern United States, the magnitude of simulated CO is consistent with observations within ±20 ppb (mean bias less than 20%). This evaluation indicates that our model generally captures the spatially and temporally averaged CO distributions. Evaluation of the CO simulation along specific flight tracks that sampled enhanced outflows during the INTEX-NA period is shown in section 4.

[14] The hourly CO mixing ratios used to sample along the flight track were not archived from the 15 year MOZART-2 simulation, preventing us from comparing this simulation directly with observations in Figure 2. Instead, we compare the regional mean CO profiles during July 2004 over the eastern United States (for land boxes within the black lines in Figure 1) from our two simulations. These regional mean CO profiles are similar both in shape and in magnitude to within ±10 ppb (not shown).

3. Identifying Strong Daily Export Events

[15] Previous studies argue that export from North America is highly episodic due to the passage of cold fronts [e.g., *Merrill and Moody*, 1996; *Cooper et al.*, 2001]. However, a cyclone passage will not necessarily lead to strongly enhanced outflow. For example, a cyclone following shortly after a previous cyclone will not generate strong outflow if the boundary layer pollutant load is low due to the previous export event. In addition, the strength and location of cyclones will affect the intensity of pollutant export from North America. Therefore, the passage of migratory cyclones alone will not necessarily predict strong export days. Instead, as described below, we use daily CO fluxes through the major export pathway (section 3.1) from the United States as simulated by the MOZART-2 model to estimate the amount of pollutant that is exported to the global atmosphere on "strong export days" versus that on other days (section 3.2).

3.1. Major Export Pathway for U.S. Pollution in Summer

[16] To identify the dominant export pathway from the United States, we first construct a monthly mean budget for North American Fossil Fuel (NAFF) CO for the continental U.S. region (24–48°N, 127.5–67.5°W, surface to 200 hPa) in July 2004. This domain is similar to those used in previous U.S. pollutant budget studies [*Horowitz et al.*, 1998; *Liang et al.*, 1998; *Pierce et al.*, 2007]. We find that most export of NAFF CO from the United States in summer occurs through the east boundary (i.e., 67.5°W) and the eastern part of the north boundary (80–67.5°W, 48°N): 5.2 Tg NAFF CO is exported through these two boundaries, compared to 0.2 and 0.4 Tg export through the 200 hPa surface and through the rest of the north boundary (Table 1). Hereafter, we refer to these two boundaries collectively as the "northeast boundary." A similar budget for total CO over the United States also shows that the northeast boundary is its major export pathway: export through this boundary is 28.5 Tg, much stronger than the vertical export (0.7 Tg through the 200 hPa surface) while the lateral transport through the remaining boundaries (the rest of the north boundary, the south boundary and the west boundary) are inflows (4.5 Tg, 4.6 Tg and 13.1 Tg, respectively, Table 1). Previous analyses are consistent with dominant export through the northeast boundary, associated with cyclones traversing the polluted regions of the United States during summers [e.g., *Merrill and Moody*, 1996; *Kiley and Fuelberg*, 2006a].

[17] The export of the NAFF CO tracer through the major transport pathway is less than 20% of that of total CO, reflecting other important CO sources in the model. Indeed, the NAFF and NABB CO tracers together, CO produced by methane oxidation, and the combined influence of fossil fuel and biomass burning sources from the other 8 source regions (also tagged in the INTEX-NA simulation, namely Europe, Africa, Australia, East Asia, South Asia, South America, Southeast Asia, India), each contribute around 20% to total CO export through this pathway. Isoprene oxidation is an important source of CO [*Duncan et al.*, 2007; *Griffin et al.*, 2007], accounting for up to another 20% of CO export (see Appendix A), with the remainder likely produced from oxidation of anthropogenic NMHC (estimated to be around 20% of the direct anthropogenic CO emission globally [*Duncan et al.*, 2007]).

[18] Despite the magnitude difference, the daily export flux time series of total CO and NAFF CO through this pathway are highly correlated ($r > 0.9$, Figure 3) and are driven by the same synoptic meteorology (discussed in section 5). Therefore, total CO can serve as a tracer to examine the variability of pollutant export from the United States in the 15 year simulation, in which NAFF CO tracer is not tagged.

3.2. Defining Strong Daily Export Events

[19] The distribution of simulated daily total CO flux through the northeast U.S. boundary for the summers of 1990 through 2004 (total of $92 \times 15 = 1380$ samples) is approximately Gaussian with a mean export (μ) of 1100 Gg CO day^{-1} and a standard deviation (σ) of 490 Gg CO day^{-1} (Figure 4). Since we wish to identify anomalously strong export events, we could label values above the mean plus one standard deviation as positive anomalies, a common practice for near-Gaussian distributions. But interannual and seasonal variation would likely mask the synoptic-scale variability we wish to examine. For example, if one summer experiences a particularly weak mean export, the use of a

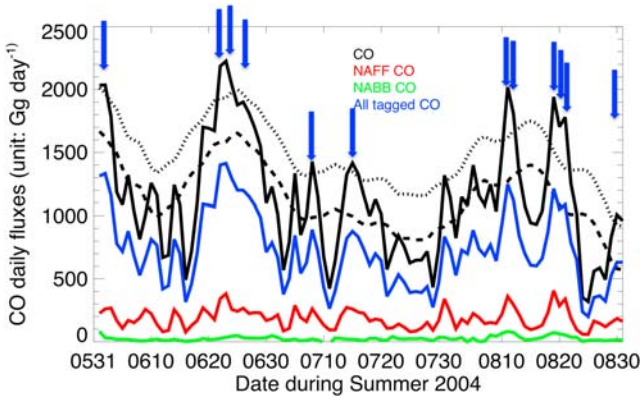

Figure 3. Daily CO (black), NAFF CO (red), NABB CO (green) and all tagged CO (including regional tagged CO and CO produced from methane oxidation, blue) fluxes (unit: Gg CO day^{-1}) through the northeast U.S. boundary (defined in section 3.1, shown in Figure 6) during the summer of 2004 in the INTEX-NA simulation. The dashed black line shows the synoptic CO flux background (15 day moving average), while the dotted black line denotes one standard deviation above the synoptic background CO flux. Arrows denote strong export days (see section 3 for details) as determined from the 15 year simulation and do not necessarily match exactly with the days above the dotted black line since the CO flux time series shown here is from the INTEX-NA simulation. The corresponding CO flux time series in the 15 year simulation has a higher daily mean flux compared to the mean daily fluxes from the INTEX-NA simulation (1290 versus 1100 Gg day^{-1}); the threshold of one standard deviation is determined from daily fluxes over 15 summers (386 Gg day^{-1}, defined as in section 3.2), while the dotted line here shows the 15 day moving average plus one standard deviation only determined by daily fluxes from the summer of 2004 (350 Gg day^{-1}, defined as in section 3.2, but with only 92 daily flux data points during that summer).

15 year mean and standard deviation would lead us to conclude that there are no strong export days during that summer. Thus, we define a "synoptic background" $[\mathbf{X}]_\mathbf{i}$ as the 15 day moving average,

$$[\mathbf{X}]_\mathbf{i} = \frac{1}{15}\sum_{\mathbf{k}=\mathbf{i}-7}^{\mathbf{i}+7} \mathbf{X_k} \tag{1}$$

where $\mathbf{X_i}$ is the total CO flux through the northeast U.S. boundary on day *i*. "strong export days" can then be defined relative to this synoptic background. We choose a threshold of one standard deviation above the synoptic background such that "strong export days" are those when $\mathbf{X_i} > [\mathbf{X}]_\mathbf{i} + \Delta\mathbf{X}$, where

$$\Delta\mathbf{X} = \sqrt{\frac{1}{92\times 15}\sum \left(\mathbf{X_i} - [\mathbf{X}]_\mathbf{i}\right)^2} \tag{2}$$

From the distribution in Figure 4, $\Delta\mathbf{X}$ = 386 Gg CO day^{-1}.

[20] Using this method, we identify 221 "strong export days" (16% of all summer days) during 1990–2004. These days contribute 25% to the total export through the northeast boundary. This contribution is consistent with that derived from a Gaussian distribution with the same relative standard deviation (σ/μ = 0.4) as our simulated daily CO fluxes (black dashed line in Figure 4; see Appendix B). The 15 year simulation contains 12 "strong export days" during the summer of 2004, on which export accounts for 20% of that summer's total export. In order to maintain a consistent definition of strong export days and to take advantage of the "idealized" 15 year simulation in which variability is induced by meteorology alone, we continue to use the strong export days diagnosed by the 15 year simulation for the INTEX-NA period during the summer of 2004. To examine export processes and evaluate with the aircraft observations, however, we use the "real" INTEX-NA simulation sampled on these strong export days diagnosed by the 15 year simulation during the INTEX-NA period in the summer of 2004 (section 4). Afterwards, we examine the sensitivity of our results to various choices we have made and identify the synoptic meteorological fields associated with strong export days (section 5).

4. Strong Export Days During the INTEX-NA Campaign

[21] In this section, we use results from the INTEX-NA simulation and observations during the INTEX-NA field campaign to examine case studies and address the ability of the model to capture the processes controlling strong daily export. Comparing the INTEX-NA simulation with the 15 year simulation for the summer of 2004, we find that, although different CO emissions lead to different mean CO export during this time period (CO daily export is 1290 versus 1100 Gg CO day^{-1} from the 15 year simulation and the INTEX-NA simulation, respectively), the daily CO fluxes in the two simulations are highly correlated (r = 0.99) due to similar meteorology (even though the INTEX-NA simulation uses NCEP/GFS meteorology while the 15 year simulation

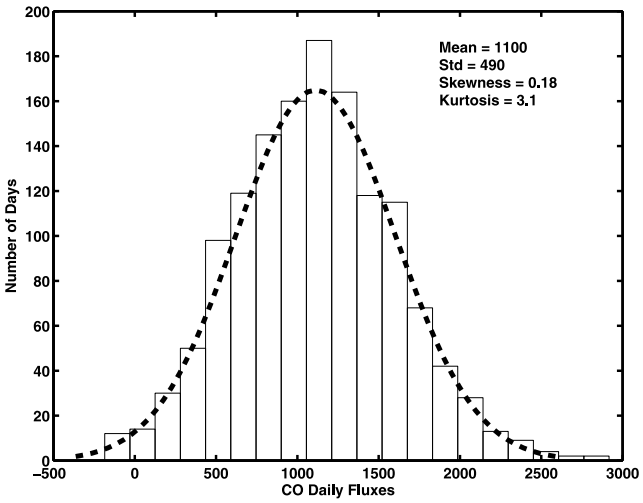

Figure 4. White bars represent the histogram of daily CO fluxes (unit: Gg CO day^{-1}) through the northeast boundary (defined in section 3.1) from 15 summers. Black dotted curve represents a Gaussian distribution with the same mean and standard deviation with the statistics shown.

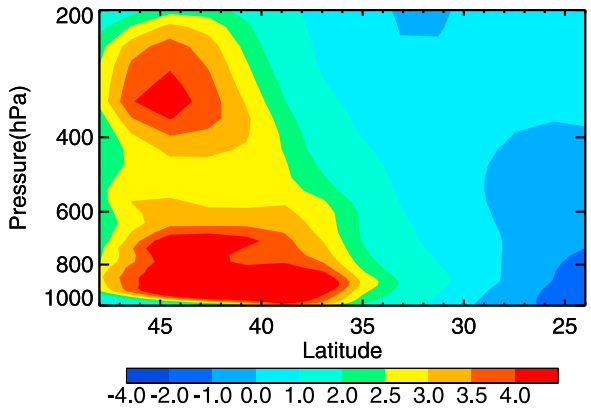

Figure 5. Latitude-pressure cross section of CO fluxes (unit: 10^{-9}moles sec^{-1} cm^{-2}) through the east boundary (67.5°W) of the United States in the INTEX-NA simulation on July 16, 2004. Positive flux indicates export through this boundary.

uses NCEP reanalysis). Applying the diagnosed 12 strong export days from the 15 year simulation to the INTEX-NA simulation, we obtain similar export contributions (20%) for CO on these days in the INTEX-NA simulation, consistent with the high correlation between the 15 year simulation and the INTEX-NA simulation discussed above. There is also a strong correlation between the NAFF CO and CO daily export fluxes simulated in the INTEX-NA simulation ($r > 0.9$, Figure 3), suggesting that the same meteorology drives the export of both tracers. During the INTEX-NA period, 4 strong export days are identified by the method described in section 3.2: July 8, July 16, August 11 and August 12 as denoted in Figure 3. We focus below on the July 16 and Aug 11–12 events; the event on July 8 is similar to that on July 16 with a low pressure system located a little further south.

4.1. July 16: Boreal Fire and Anthropogenic Signals

[22] On July 16, a midlatitude cyclone was located over the Maritime Provinces of Canada, carrying a cold front extending southwestward along the east coast of the United States. The dominant surface wind close to the northeast U.S. boundary (defined in section 3.1) was southwesterly. Strong surface export of CO occurred mostly through the east boundary at latitudes of 35–48°N (Figure 5). Meanwhile, a warm conveyor belt (WCB) lifted surface CO to the middle and upper troposphere, which, combined with the southwesterlies near the boundary due to an upper level trough, resulted in a region of high CO flux in the free troposphere centered at 44°N through this boundary (Figure 5). Based on the circulation, pollutants exported through the east boundary on July 16 would have been transported in southwesterly flow at the surface and in the upper troposphere. The flight track two days later (July 18) covered the region to the northeast of the boundary (Figure 6), providing an opportunity to evaluate the simulated export.

[23] The simulated distribution of CO at 950 hPa on July 16–18 is shown in Figure 7. Export can be seen to occur in these snapshots: an intense CO plume existed on July 16 over the northeastern United States, and was advected northeastward on the following days until sampled by the NASA DC-8 flight on July 18. According to the model, at around 14:30, 16:00, 20:30 and 22:00 UTC, the intense CO plume should have been sampled in the boundary layer while at 18:00 UTC, the flight should have sampled the edge of this plume. A comparison between the simulated and observed CO mixing ratios measured along the flight track is shown in Figure 8. Our simulation captures the high CO mixing ratios (>150 ppb) at these times within that plume, but with an overestimate of 50–100 ppb near Maine, which is close to the source region (around 14:30 UTC, 22:00 UTC), consistent with an overestimate of CO emissions from the United States in the NEI99 emission inventory [*Hudman et al.*, 2007, 2008]. The simulated high CO mixing ratios near the surface are dominated by the NAFF tracer of anthropogenic pollution (Figure 8). This anthropogenic plume is consistent with the strong export flux in the lower troposphere two days earlier (July 16, Figure 5).

[24] The simulated upper tropospheric distribution of CO on the flight day (July 18, Figure 9) shows two strong plumes: one located near the Gulf of Maine and Canadian Maritimes, and the other to the north of this region. The flight intersected the plume before 14:00 UTC over Maine, at around 15:00 UTC over the Gulf of Saint Lawrence and at 21:00 UTC over Nova Scotia with CO mixing ratios around 100–120 ppb (in both observations and the model, Figure 8). Later, when the plane flew over the Gulf of Saint Lawrence to the east at around 17:00 UTC, both observed and simulated CO decreased to below 100 ppb, implying that the flight moved to the edge of this plume, and that the model resolves the spatial extent of the plume. In the model, this CO plume at 380 hPa on July 18 mainly follows the spatial pattern of the NAFF anthropogenic tracer and is due to lifting of surface pollutants by the WCB airstream, as evidenced by the strong flux through the northeast U.S. boundary on the previous day (July 16, Figure 5). The northern plume at 380 hPa in our model contained CO mixing ratios as high as 100 ppb. However, observations at the same location sampled extremely high CO (in excess of

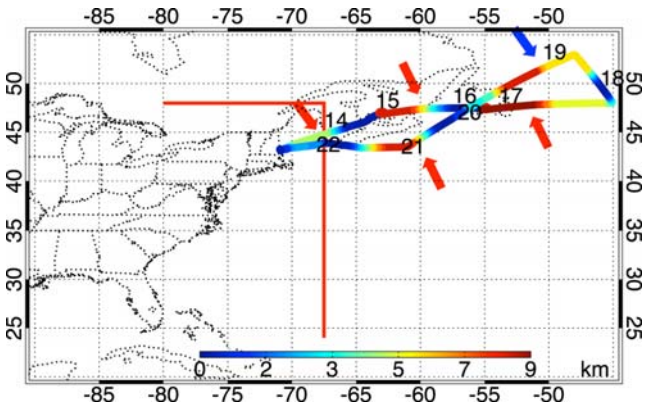

Figure 6. The flight track on July 18, 2004. Gray scale shows flight altitude (unit: km). Black solid lines denote the "northeast boundary" of the United States; White arrow shows the location where the strongest CO signals were sampled. Black arrows represent the times when elevated CO concentrations in the middle and upper troposphere were sampled. Numbers along the flight track show the time (UTC) when the plane sampled air at that location.

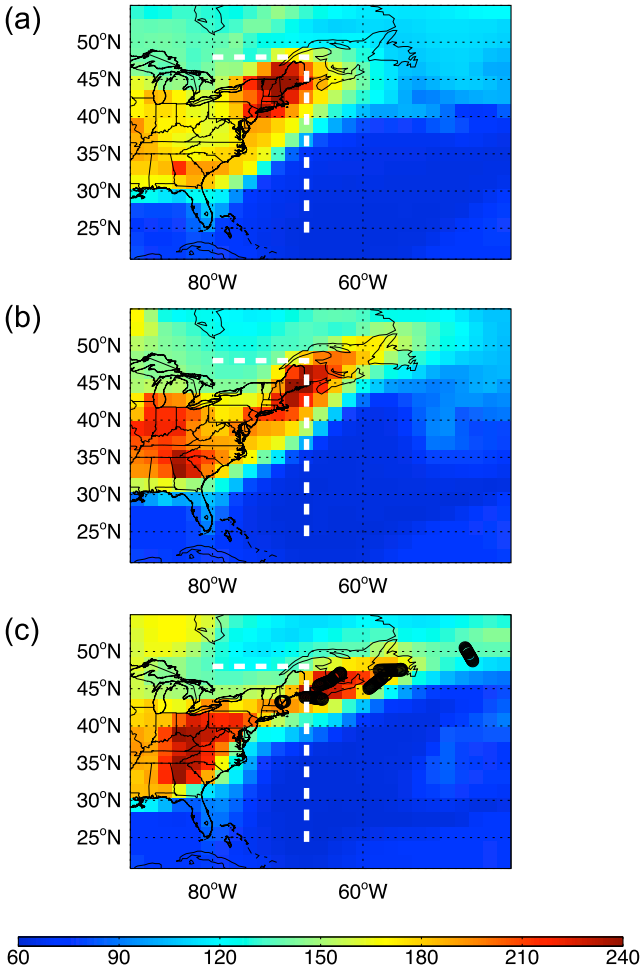

Figure 7. The daily average CO distribution (unit: ppbv) from the INTEX-NA simulation at 950 hPa on July (a) 16, (b) 17, and (c) 18. White dashed lines represent the northeast boundary of the United States we choose to calculate our CO export fluxes; open circles represent the location of aircraft measurements between 0 and 2 km (July 18 only).

500 ppb) at about 19:00 UTC. In the model, the NABB CO tracer has a greater contribution (up to 35 ppb) to this plume than the NAFF CO tracer (Figure 8). The summer of 2004 was one of the largest fire seasons on record in North America due to persistent wildfires in the boreal forests of Alaska and Canada [*Fuelberg et al.*, 2007]. The high CO mixing ratios (up to 500 ppb) sampled downwind by the DC-8 flight at 4–9 km indicates that very limited dilution occurred [*Singh et al.*, 2006]. Previous studies suggest strong pyroconvective events associated with these fires, injecting pollutants from biomass burning into the middle and upper troposphere [*Turquety et al.*, 2007; *de Gouw et al.*, 2006]. Our biomass burning emissions are distributed up to 4 km with 70% of these emissions occurring below 2 km [*Horowitz et al.*, 2007]. The lower CO mixing ratios in our model likely reflect an underestimate in this injection height or excessive dilution of the fire plume.

[25] We conclude that the model is able to capture the location and timing of the plume associated with anthropogenic outflow on July 18. The model also captures the

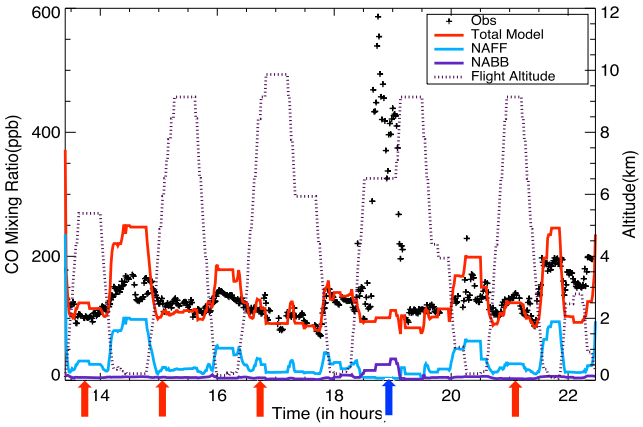

Figure 8. CO mixing ratios (unit: ppbv) along the flight track on July 18, 2004, in the observations (black) and in the model total CO (red), CO from North American fossil fuel (NAFF, blue), CO from North American biomass burning (NABB, purple). The dashed gray line is the flight altitude (unit: km). The white arrow shows the extreme CO signal (see also Figure 6). Black arrows represent the times when the flight sampled elevated CO concentrations in the middle and upper troposphere (see also Figure 6).

location, but underestimates the magnitude of the observed biomass burning plume in the upper troposphere.

4.2. August 11–12: Influences From Fronts and WCB Lifting

[26] In the model, August 11 and August 12 are strong export days, while the NASA DC-8 flight was conducted on August 11. The main objectives of this flight were to sample North American outflow to the Atlantic, investigate WCB lifting and sample concentration changes across the cold front [*Singh et al.*, 2006].

[27] On August 11, a midlatitude cyclone was centered to the south of Hudson Bay. A quasi-stationary cold front associated with this cyclone extended southwestward to Texas. East of the front, warm air streamed northeastward. Pollutants emitted from the surface were lifted ahead of the front by the WCB air stream to the middle and upper troposphere. The flow in the middle and upper troposphere was dominated by a strong closed low near the Great Lakes

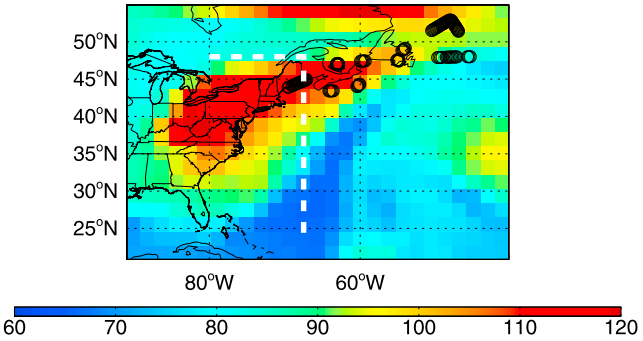

Figure 9. The daily average CO distribution (unit: ppbv) from the INTEX-NA simulation at 380 hPa on July 18. White dashed lines represent the northeast boundary of the United States; open circles represent the location of aircraft measurements between 6 and 8 km.

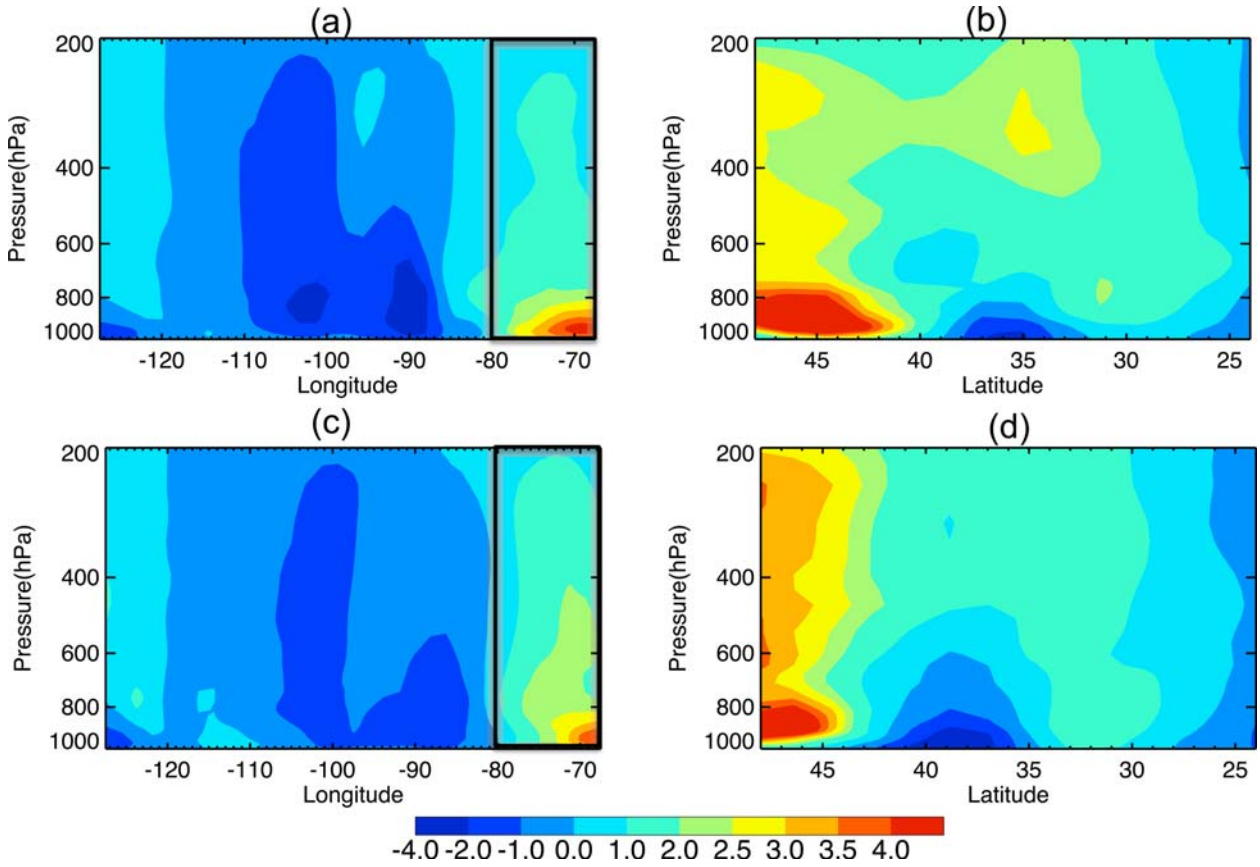

Figure 10. (a and c) Longitude-pressure cross section of CO fluxes (unit: 10^{-9} mole sec^{-1} cm^{-2}) through the north boundary (48°N) and (b and d) latitude-pressure cross section through the east boundary (67.5°W) on (top) August 11 and (bottom) August 12, 2004, in the INTEX-NA simulation. The black rectangle represents the part of the north boundary included in the northeast boundary used to identify high export days (section 3).

and an associated trough that extended southward from it (http://cloud1.arc.nasa.gov/intex-na/flight_reps.html). Under this situation, strong export fluxes of CO through the north and the east boundaries of the United States occur in the surface level and throughout the free troposphere (Figures 10a and 10b). As the weather system moved northeastward on August 12, more CO was exported across the north boundary than on the previous day (Figures 10c and 10d). The upper tropospheric trough moved faster than the surface low pressure system, approaching the northeast boundary. The stronger pressure gradient near the trough caused stronger southwesterly flow, which, combined with the previously lifted surface pollutants, led to stronger CO export through the eastern part of the north boundary (Figure 10c) and through the northern part of the east boundary (Figure 10d) relative to the previous day. Compared to the July 16 case (Figure 5), the cyclone system on August 11–12 was located further west, and hence a larger portion of the export passed through the north boundary.

[28] The flight on August 11 serves to check the pollutant export resulting from the frontal passage. A plume with enhanced CO concentration (and enhanced NAFF CO tracer) was simulated along the east coast at 950 hPa in the model (Figure 11a), consistent with the strong CO fluxes through the east boundary, located at around 45°N at the surface level (Figures 10a and 10b). Corresponding to this strong export, the flight sampled a plume with CO mixing ratios near 180 ppbv at around 13:00 UTC to the east of our east boundary (Figure 12). At 380 hPa, a strong plume extended offshore along the eastern coast of the United States and to the east of the surface cold front (Figure 11b), with enhanced NAFF CO tracer. This elevated plume was sampled once at around 14:00 UTC. At that time, according to our simulation, the NASA DC-8 sampled higher CO concentrations as it climbed to higher altitude, following the trend of the NAFF CO tracer and reflecting the WCB lifting of surface pollutants (Figure 12). Throughout the entire flight track on August 11, the NAFF CO tracer (Figure 12) accounts for much of the observed variability, especially before 18:30 UTC, implying an effect from WCB lifting to the east of the cold front. After 18:30 UTC, the flight crossed the cold front in the boundary layer between the border of Virginia and Kentucky, showing much lower CO mixing ratios behind the cold front, as captured by the model (Figures 11a and 12). This comparison shows that our model captures the export associated with the cyclone passage and the WCB lifting.

[29] In addition to the DC-8 observations, a consistent picture of export on these days emerges from an animation of pollutant export that the NOAA Aeronomy Laboratory produced for the ICARTT community (http://www.esrl.noaa.gov/csd/metproducts/icartt2004/archive/movies/ICARTT_CO_NA_00km_20km.mov) using the FLEXPART

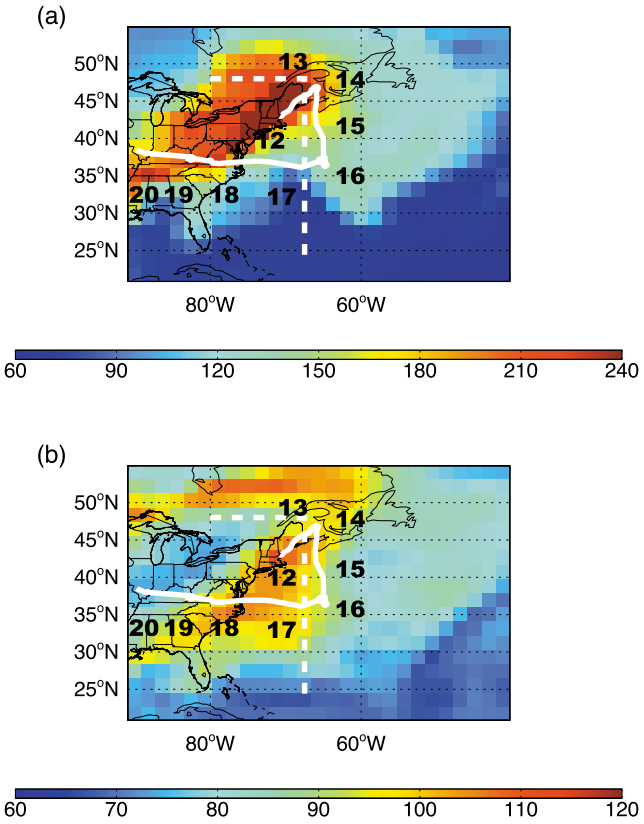

Figure 11. Simulated CO distribution (unit: ppbv) at (a) 950 hPa and (b) 380 hPa on August 11. White dashed line show the northeast boundary of the United States; white solid line shows the flight track; black numbers show the time (UTC) along the flight track.

Lagrangian Particle dispersion model [*Owen et al.*, 2006, and references therein] and from MOPITT CO columns for this time period (data processed from MOPITT level 2 data as in work by *Fang et al.* [2005] (not shown)).

5. Contribution of Strong Export Days to Total U.S. Pollutant Export

[30] In section 3.2, we found that strong export days occur on 16% of all summer days (221 days) and account for 25% of total summertime export from 1990 to 2004. Clearly, the remaining summer days play a nonnegligible role in total pollutant export. We further separate these remaining days into two categories: "moderate" and "weak" export days, defined as the days on which the CO flux through the northeast boundary exceeds the synoptic background (15 day running mean) by less than one standard deviation, and days when this flux is below the synoptic background, respectively. We find that there are 466 moderate export days (34% of all summer days) and 693 weak export days (50% of all summer days), contributing 40% and 35% to total export, respectively.

[31] Next, we examine the sensitivity of the contribution from strong export days to total export to various assumptions in our approach (section 5.1). We also identify the meteorological patterns associated with different categories of export days (section 5.2).

[32] Finally, we extend our analysis to consider export during springtime (section 5.3).

5.1. Sensitivity Analysis

[33] First, we test the sensitivity of our conclusions to the choices of different boundaries used to calculate CO export fluxes from the United States. In addition to the northeast boundary (section 3.1) used so far in our analysis, we consider here an east boundary only (24–48°N, 67.5°W) and an extended east boundary (24–55°N, 67.5°W). We find that the distributions of daily CO fluxes through these different boundaries during the 15 summers are still close to Gaussian distributions with σ/μ also around 0.4, yielding a similar contribution from strong export days (25–26%). While the major conclusions are robust to the choice of boundary, the northeast boundary of the U.S. is most suitable because it captures most of the export of anthropogenic pollution from the contiguous United States (plus part of southern Canada) while avoiding strong influences from the biomass burning prevalent in Alaska and Canada during the summer of 2004.

[34] If we reduce the averaging period of the running mean used to estimate the synoptic background from 15 to 7 days, the number of strong export days during the 15 summers decreases slightly, from 221 to 216 days (still 16% of all summer days). The contribution of strong export days to total summertime export through the northeast U.S. boundary decreases to 22% (as compared to 25% for a 15 day running mean). While we choose to classify export days relative to a "synoptic background," the absolute magnitude of the pollutant export flux is likely more important for downwind impacts. Therefore, we also examine the sensitivity of our findings to defining the threshold from the 15-summer mean as well as the summer mean of each individual year. In both cases, the contribution from strong daily export events to total export is within the range of 22–26% on about 16% of all summer days.

[35] When the above changes in boundaries or averaging period are applied, "strong daily export" still occurs on close to 16% of days, reflecting the Gaussian distribution of the summer daily fluxes. Additionally, the intrinsic statistics of our CO daily export fluxes (a modest relative standard

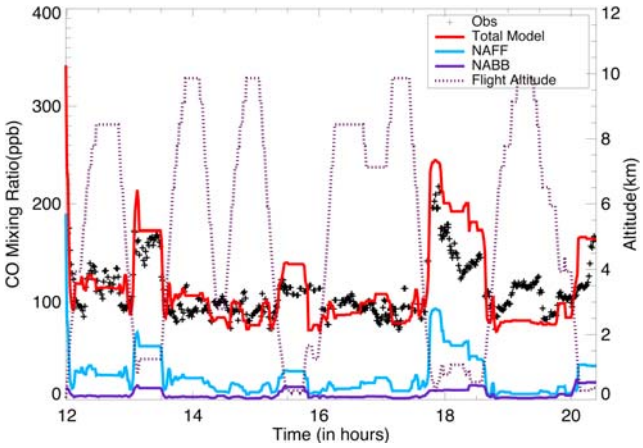

Figure 12. CO mixing ratio (unit: ppbv) comparison along flight track on August 11, 2004; also shown are the North American anthropogenic CO tracer (NAFF, blue) and biomass burning CO tracer (NABB, purple).

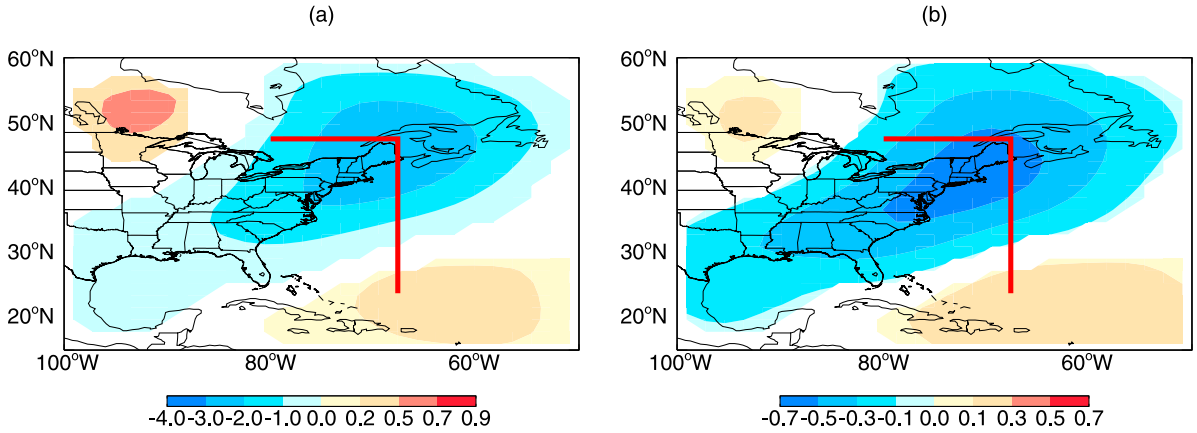

Figure 13. (a) Regression slope (unit: hPa per standard deviation change of CO flux anomalies) and (b) correlation coefficient of the daily surface pressure anomalies on the daily anomalies of the total CO fluxes through the northeast boundary of the United States (defined as in section 3.1, a plane along 67.5°W, from 24 to 48°N, extending from the surface to 200 hPa, and the eastern part of the north boundary, a plane along 48°N, extending from 80 to 67.5°W, from the surface to 200 hPa, shown in black lines) during the summers of 1990–2004. Anomalies are calculated relative to a 15 day running mean that defines the synoptic "background" values. Only those values with 95% confidence (f test) are shown.

deviation of 0.4) directly determine that the contribution of strong export to the total export cannot exceed 30% if we continue to use one standard deviation as a threshold for defining strong export days. That is to say, the daily CO fluxes would have to exhibit a much wider distribution (relative standard deviation greater than 1.4) for strong export days to dominate the total export.

[36] We also test the sensitivity of our results to the use of total CO (as compared with NAFF CO) as a tracer for pollutant export from North America in the summer of 2004. Using the same methodology for NAFF CO during this summer in the INTEX-NA simulations yields a similar contribution from strong export days to the total export of NAFF CO (22%), consistent with the high correlation coefficient between NAFF CO and CO export fluxes (section 3.1 and Figure 3). The correspondence between total CO and NAFF CO confirms that our use of total CO fluxes from the 15 year simulation accurately represents the export of U.S. pollution.

[37] Finally, the one standard deviation threshold identifies only the strongest daily export events relative to the synoptic background. If we relax the one standard deviation threshold to include all days on which export is above the synoptic background (i.e., strong export days and moderate export days, 50% of all summer days), these days contribute 65% of total export. The remaining days (weak export days, 50% of all summer days) still account for 35% of total export. These numbers are consistent with those derived from an idealized Gaussian distribution (see Appendix A).

5.2. Meteorological Patterns Associated With Different Export Categories

[38] We examine how the variability in the total CO export flux through the northeast boundary is driven by meteorology (represented here by surface pressure) within the 15 summers of our simulation. In order to focus on the synoptic variability, we remove seasonal changes in export by first defining the "synoptic background" (15 day moving average) values for surface pressure (as we did for CO fluxes in section 3.2). We then regress the daily surface pressure anomalies relative to these synoptic background values on the daily CO flux anomalies. Strong CO fluxes through the northeastern U.S. boundary are associated with a low pressure center over the Gulf of Saint Lawrence (Figure 13). CO flux anomalies of one standard deviation above the background are associated with a low-pressure anomaly of 2 to 3 hPa. While correlation coefficients are high (up to 0.7), ~50% of the variability is *not* captured, suggesting a role for other processes and synoptic conditions in ventilating U.S. pollution. Identification of these processes requires further study, but they likely include the westward extension of the Bermuda High and convection [e.g., *Li et al.*, 2005; *Auvray and Bey*, 2005; *Owen et al.*, 2006]. Regressing the surface pressure anomalies on the NAFF CO export flux anomalies during the summer of 2004 shows a similar pattern, indicating that the synoptic scale variability of the NAFF CO fluxes and total CO fluxes is indeed driven by the same meteorological processes.

[39] Additionally, we construct a composite of the surface pressure anomalies (relative to the 15 day running mean background values) that occur on "strong export days," "moderate export days" and "weak export days" as defined in section 5. Strong export days are clearly associated with migratory midlatitude cyclones (Figure 14a), consistent with Figure 13 and prior studies [e.g., *Merrill and Moody*, 1996; *Stohl*, 2001; *Wild and Akimoto*, 2001].

[40] The low pressure system over Gulf of Saint Lawrence also emerges in Figure 14b, suggesting that some cyclones are associated with moderate daily export. According to *Fuelberg et al.* [2007], cyclone passages were more frequent than normal during the summer of 2004 relative to other years. If all cyclones led to strong export, we would expect that the strong export days and the contribution of export during these days would be higher than in the other

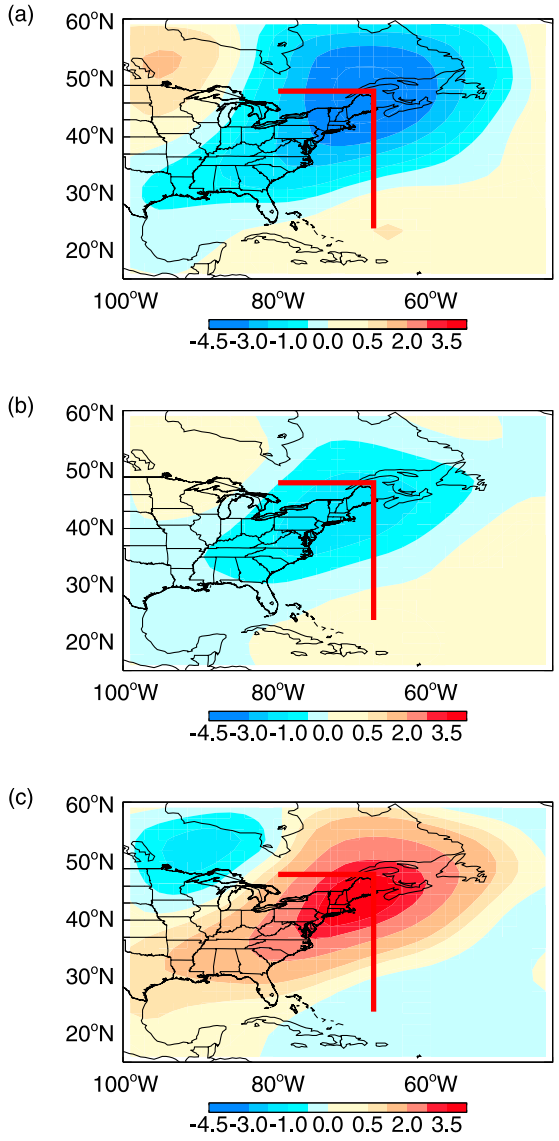

Figure 14. Composite of surface pressure anomalies (hPa) relative to the 15 day moving average "background" values for (a) strong, (b) moderate, and (c) weak export days, defined as described in section 5. Black lines show the northeast boundary of the United States. The number of days (from 15 summers of 1990 to 2004) included are: 221 (16%, Figure 14a), 466 (34%, Figure 14b), and 693 (50%, Figure 14c) days, contributing 25%, 40%, and 35%, respectively, to total summertime export through the northeast boundary.

years. However, when we compare our estimate for the summer of 2004 to all 15 summers (1990–2004), the number of strong export days and the strong export contribution to the total export are both below average (13% and 20% for the summer of 2004 versus 16% and 25% for all summers, respectively).

[41] The fact that some cyclones only lead to moderate export may also explain the apparent differences between our work and previous studies. For example, *Kiley and Fuelberg* [2006b] studied summer time transport plumes during the INTEX-NA campaign period. They considered two cases of export of anthropogenic plumes from the northeast United States (July 19 and August 2–5), both of which experienced cyclone passages. For comparison, the NAFF CO column burdens on July 16 (a diagnosed strong export day) and July 19 are both shown in Figure 15. We see that our model does capture localized export on July 19. However, the cyclone passage on July 19 follows closely the July 16 cyclone passage, and therefore does not generate as strong an export flux as that on July 16. Instead, strong export occurs only in a narrow region near the northern edge of our east boundary. During August 2–5, almost the whole eastern United States is dominated by a high pressure system, with only a weak frontal boundary and a low pressure area along the Atlantic Coast. Although the NAFF CO column distribution on August 4 (Figure 15c) shows that local export is occurring, the dominant feature on this day is the high NAFF column over much of the eastern United States accumulating under a high pressure system that hinders export. However, the cyclone on August 11 is much stronger and dominates the whole eastern United States, sweeping previously accumulated pollutants offshore and generating strong export fluxes (Figure 15d). As a consequence, although our model captures the anthropogenic plumes during the two cases mentioned by *Kiley and Fuelberg* [2006b], export fluxes during July 19 and August 2–5 fall into the "moderate" rather than "strong" category (Figure 4). The difference between our study and previous concentration-oriented studies during the INTEX-NA period indicates that, while focusing on concentration enhancements associated with migratory cyclones is necessary for understanding the physical and chemical evolution of pollutant transport, it does not necessarily capture the times when the export of pollutants from the United States to the global atmosphere is strongest.

[42] In contrast to the strong and moderate export days that more likely occur when a low pressure system is located over the Gulf of Saint Lawrence (Figures 14a and 14b), the composite during weak export days shows a surface high located over the Canadian Maritimes. These days contribute 35% of total export, indicating that attempting to diagnose U.S. pollutant export to the global atmosphere directly from observations taken when migratory cyclones are present over the eastern U.S. will exclude >30% of the export. We suggest that future campaigns examine other export mechanisms (e.g., westward extension of the Bermuda high and convection, particularly in the southeastern United States) in order to provide additional insights and key tests for models.

[43] If we focus on the days with the weakest export (those below one standard deviation of the 15 day running mean), we find a similar pattern as in Figure 14c except that the intensity of the high-pressure system is stronger. The contribution from these weakest export days (16% of all days) is 7% of the total export, a disproportionately small amount of the total export. The contribution per day from the weakest export days, however, is still around one fourth of that during the strongest days and thus a nonnegligible component of the total export.

5.3. Strong Daily Export Contribution During Spring

[44] Although summer is the season when photochemically active pollutants in the continental U.S. boundary layer, i.e., reactive nitrogen (NO_y) and O_3, are highest, spring

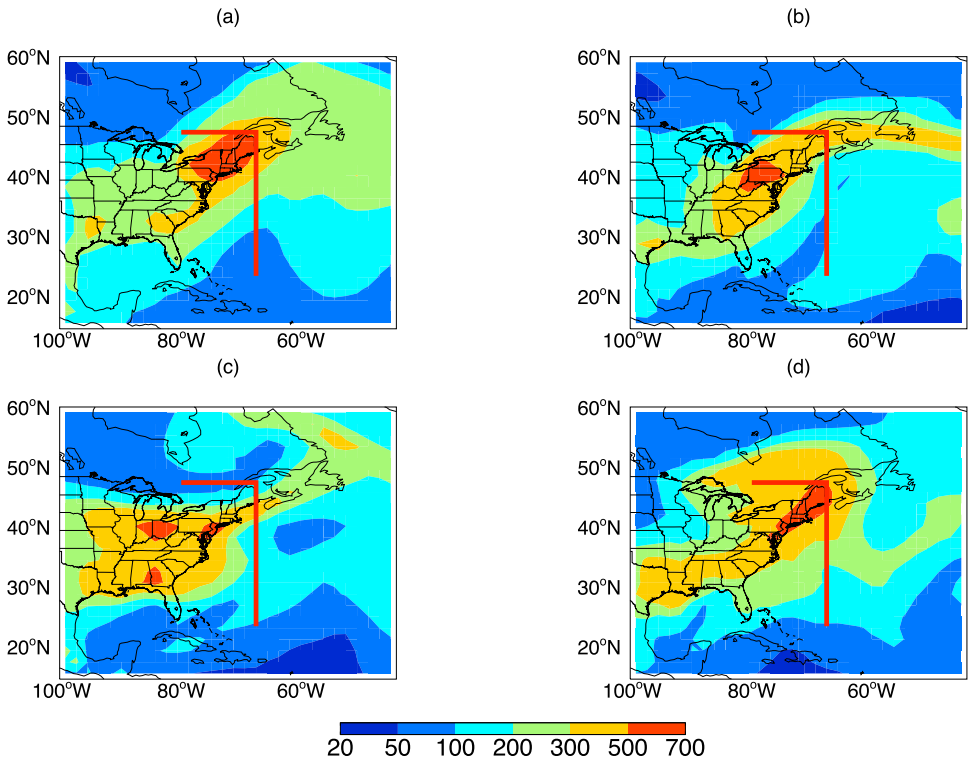

Figure 15. NAFF CO tropospheric column (unit: 10^{15} molecules cm^{-2}) over the eastern United States from the INTEX-NA simulation on (a) July 16, (b) July 19, (c) August 4, and (d) August 11. Black lines show the northeast boundary of the United States used to estimate export fluxes.

is the season with maximum pollutant export from North America, e.g., to Europe [*Auvray and Bey*, 2005]. Here, we extend our study to examine the daily export fluxes during springs. The springtime daily fluxes through the northeast boundary of the United States also follow a Gaussian distribution (the skewness and kurtosis of this data set are 0.04 and 2.9) with a mean daily flux of 2100 Gg day^{-1} and a standard deviation of 870 Gg day^{-1}. Although the springtime magnitude of the mean daily export and its standard deviation are almost double those in summer, the ratio between them (the relative standard deviation, σ/μ) is equivalent. The contribution from strong export events to total export is thus similar to that in summer, with springtime strong, moderate and weak daily export events occurring on 210 (15%), 507 (37%) and 664 (48%) days, accounting for 22%, 41% and 36% of the total pollutant export, respectively.

[45] Given this classification, we conduct a composite study of surface pressure anomalies during springtime on different export days as was done for summer in Figure 14. During springtime, strong export days are also associated with migratory midlatitude cyclones. As in summer, weak export occurring when a high-pressure system is located over the Gulf of Saint Lawrence also makes an important contribution to total export (36%), pointing to a need for additional attention on export mechanisms other than cyclone passages.

6. Conclusions

[46] Pollutant transport from the United States exhibits notable variability and is thus often considered to be "episodic," though the extent of this episodicity and the relative contribution of episodic export from the United States to the total export have not been evaluated. We apply a statistical definition based upon 15 summers of daily CO fluxes through the dominant export pathway from the eastern United States simulated with the MOZART global chemical transport model to identify strong daily export events and quantify their contribution to total U.S. pollutant export.

[47] We find that the dominant pathway by which U.S. pollutants are exported to downwind regions in summer is through the northeast boundary of the continental United States (defined in section 3.1). The distribution of simulated daily CO export fluxes through the northeast boundary from 15 summers (1990–2004) is approximately Gaussian (Figure 4). In order to focus on the synoptic variability of export, we classify the daily fluxes through the northeast boundary according to the magnitude of these daily CO fluxes relative to their 15 day moving average "synoptic background" (section 3.2) to avoid the interference of seasonal and interannual fluctuations. We identify "strong export days" (on which export exceeds the synoptic background (15 day running mean) by more than one standard deviation), "moderate export days" (on which export is above the synoptic background by less than one standard deviation), and "weak export days" (on which export is below the synoptic background). Consistent with Gaussian statistics, "strong export days" account for 16% of all days and 25% of the total export during the 15 summers. The contribution of less than 30% of total export from strong export days reflects the low value of the relative standard

deviation (ratio of standard deviation over mean), determined by the intrinsic statistics of the daily CO export fluxes. Even when we include both strong and moderate export days, i.e., all days with export above the synoptic background, the contribution to total export is 65% on 50% of all days, while the remaining 35% of export happens during the other 50% days (weak export days).

[48] Comparison of modeled CO outflow plumes with observations along specific flight tracks during the INTEX-NA field campaign in the summer of 2004 shows that the model captures the intensity and location of the observed anthropogenic plumes, except for a consistent positive CO bias close to source regions, which may reflect an overestimate of anthropogenic CO emissions [*Hudman et al.*, 2007]. We identify four strong export days during the INTEX-NA field campaign period. Comparison with observations on those days shows that the model captures the timing, location, magnitude and meteorological conditions associated with observed enhancements of CO outflow. During these events, strong surface export fluxes are associated with the passage of cyclones that generate strong southwesterlies sweeping surface pollutants offshore and strong pollutant fluxes in the free troposphere reflecting the lifting of surface pollutants by Warm Conveyor Belts (WCBs).

[49] We find that strong CO export fluxes through the northeast boundary over 15 summers are significantly correlated with the passage of midlatitude cyclones over the Gulf of Saint Lawrence, producing a cyclonic circulation and WCB lifting of surface pollutants, in agreement with previous studies showing that cyclone passages are the major driver for strong export events [e.g., *Merrill and Moody*, 1996; *Stohl*, 2001; *Wild and Akimoto*, 2001]. The correlation ($r^2 = 0.5$) between the low pressure center over the Gulf of Saint Lawrence and the daily flux anomalies through the U.S. northeast boundary (Figure 13), however, indicates that although migratory midlatitude cyclones account for a majority of the daily CO flux variability, there are other factors that affect U.S. pollutant export through the northeast boundary, possibly including cyclones in different locations, extension of the Bermuda High and convection [e.g., *Li et al.*, 2005; *Auvray and Bey*, 2005; *Owen et al.*, 2006]. For example, "weak export days" are more likely to occur in the absence of midlatitude cyclones (Figure 14c).

[50] An extension of our analysis to spring shows that although the mean daily export flux through the northeast U.S. boundary and its standard deviations are almost twice that for summer (2100 vs. 1100 Gg day^{-1} for mean daily export fluxes and 880 versus 490 Gg day^{-1} for the standard deviation), the contributions from strong, moderate and weak export days and the associated synoptic meteorological patterns are approximately equivalent. This equivalency occurs because both spring and summer daily fluxes follow a Gaussian distribution with a relative standard deviation of 0.4.

[51] We conclude that focusing exclusively on outflow plumes during cyclone passages, although critical for understanding the transport processes of pollutants from the source region, provides an incomplete picture of total U.S. pollutant export. An emphasis in future campaigns on other mechanisms (westward extension of Bermuda high and convection, particularly in the southeastern United States) would provide additional insights and key tests for models. Moreover, continuous measurements are necessary for an observationally based estimate of total pollutant export from the United States and its impact on the global atmosphere.

[52] Recent studies suggest that global warming may lead to a decrease in cyclone frequency while increasing local pollution in the northeastern United States [*McCabe et al.*, 2001; *Mickley et al.*, 2004; *Lambert and Fyfe*, 2006]. Decreasing cyclone frequency and increasing local pollution could lead to more intense strong daily export events. However, if the frequency of such events decreases, the overall contribution of strong export days to total pollutant export may not increase. Further investigation is needed to determine the impact of global change on strong daily export events from the United States.

Appendix A: Estimating CO Flux From Isoprene Emitted Within the United States

[53] Total isoprene emission within the United States is 5.3 Tg in July of 2004. To estimate the contribution of isoprene oxidation to CO export (fully simulated by our model, but not specifically tagged), we assume here a yield of CO from isoprene oxidation (α_{isop}, a yield of CO per carbon) as 0.4, a value for polluted regions from *Duncan et al.* [2007]. The source to CO from isoprene emitted within the United States is 4.3 Tg in July, almost half the total CO surface emissions in our model. Assuming this CO is all exported through the northeast wall within July, then the CO flux due to isoprene oxidation is estimated to be 4.3 Tg during July 2004 (i.e., 140 Gg day^{-1}), which represents around another "one fifth" of total CO export flux (section 3.1).

Appendix B: Strong Export Contribution to Total Export Estimated From a Gaussian Distribution

[54] Assume y is the probability density function of daily mean export flux (x) during the summers, μ is the mean summer daily flux for all 15 years and σ is the standard deviation of all the daily flux. y follows a Gaussian distribution of x,

$$y = \frac{1}{\sigma\sqrt{2\pi}} e^{-\frac{(x-\mu)^2}{2\sigma^2}} \tag{B1}$$

Then the cumulative distribution function of this idealized Gaussian distribution is

$$\int \frac{1}{\sigma\sqrt{2\pi}} e^{-\frac{(x-\mu)^2}{2\sigma^2}} dx = -\frac{1}{2}\mathrm{erf}\left(-\frac{x-\mu}{\sigma\sqrt{2}}\right) \tag{B2}$$

Strong export days are those days with CO flux greater than $\mu + \sigma^{\mu+\sigma}$. If we integrate (B2) from $\mu + \sigma$ to $+\infty$, we obtain the percentage of strong export days over all days. The result is

$$\frac{1}{2} + \frac{1}{2}\mathrm{erf}\left(-\frac{1}{\sqrt{2}}\right) = 0.16 \tag{B3}$$

This 16% is directly determined by the fact that the summer daily CO export flux data set follows a Gaussian distribution.

[55] To calculate the contribution from strong daily export events to the total export, we integrate the following function,

$$\int y^*x^*dx = \int \frac{1}{\sigma\sqrt{2\pi}} e^{-\frac{(x-\mu)^2}{2\sigma^2}}$$

$$x^*dx = \frac{-e^{-\frac{(x-\mu)^2}{2\sigma^2}}\sigma^2 - \mu\sigma\sqrt{\frac{\pi}{2}}\mathrm{erf}\left(-\frac{x-\mu}{\sigma\sqrt{2}}\right)}{\sigma\sqrt{2\pi}} \quad \text{(B4)}$$

If we integrate (B4) from $-\infty$ to $+\infty$, we obtain the ratio of the total export divided by the number of all the days (i.e., mean value of these daily fluxes):

$$\frac{\mu\sqrt{\frac{\pi}{2}}}{\sqrt{2\pi}} + \frac{\mu\sqrt{\frac{\pi}{2}}}{\sqrt{2\pi}} = \mu \quad \text{(B5)}$$

Instead, if we integrate (B4) from $+\infty$ to $+\infty$, we obtain the ratio of strong daily export over the number of all days,

$$\frac{\mu}{2} + \frac{\mu}{2}\mathrm{erf}\left(-\frac{1}{\sqrt{2}}\right) + \frac{\sigma e^{-\frac{1}{2}}}{\sqrt{2\pi}} = \frac{\mu}{2}\left(1 - \mathrm{erf}\left(\frac{1}{\sqrt{2}}\right)\right) + 0.242\sigma = 0.16\mu + 0.24\sigma \quad \text{(B6)}$$

Then, the contribution of strong export to total export (rs, ratio of strong export over the total export) is then

$$rs = \frac{0.16\mu + 0.24\sigma}{\mu} = 0.16 + 0.24\frac{\sigma}{\mu} \quad \text{(B7)}$$

Similarly, we integrate (B4) from μ to $\mu + \sigma$ to calculate the ratio of moderate daily export over the number of all days,

$$-\frac{\mu}{2}erf\left(-\frac{1}{\sqrt{2}}\right) + \frac{\sigma}{\sqrt{2\pi}} - \frac{\sigma e^{-\frac{1}{2}}}{\sqrt{2\pi}} = 0.34\mu + 0.16\sigma \quad \text{(B8)}$$

The contribution of moderate export to total export (rm, ratio of moderate export over the total export) is then

$$rm = \frac{0.34\mu + 0.16\sigma}{\mu} = 0.34 + 0.16\frac{\sigma}{\mu} \quad \text{(B9)}$$

Finally, the remaining weak export contribution (rw) is

$$rw = 0.5 - 0.4\frac{\sigma}{\mu} \quad \text{(B10)}$$

[56] From our summer daily CO export flux data set, μ = 1100 Gg CO day^{-1} and σ = 490 Gg CO day^{-1}, yielding σ/μ = 0.4. Therefore, our estimated rs, rm and rw from corresponding Gaussian distribution will be 26%, 40% and 34%. This estimation is consistent with our calculation in section 3, suggesting that the intrinsic feature of the summer daily CO export fluxes (close to a Gaussian distribution with a relative standard deviation of 0.4) directly determines that export during the strong export days accounts for less than 30% of total export. Similar derivation can be applied to the spring daily fluxes during the 15 years, from which σ/μ is also around 0.4.

[57] **Acknowledgment.** We thank all the anonymous reviewers for comments on earlier versions of the manuscript that have greatly helped to improve this paper.

References

Auvray, M., and I. Bey (2005), Long-range transport to Europe: Seasonal variations and implications for the European ozone budget, *J. Geophys. Res.*, *110*, D11303, doi:10.1029/2004JD005503.

Bey, I., D. J. Jacob, R. M. Yantosca, J. A. Logan, B. D. Field, A. M. Fiore, Q. Li, H. Y. Liu, L. J. Mickley, and M. G. Schultz (2001), Global modeling of tropospheric chemistry with assimilated meteorology: Model description and evaluation, *J. Geophys. Res.*, *106*, 23,073–23,095, doi:10.1029/2001JD000807.

Cooper, O. R., J. L. Moody, D. D. Parish, M. Trainer, J. S. Holloway, T. B. Ryerson, G. Hubler, F. C. Fehsenfeld, S. J. Oltmans, and M. J. Evans (2001), Tracer gas signatures of the airstreams within North Atlantic Cyclones: Case studies from the North Atlantic Regional Experiment (NARE'97) aircraft intensive, *J. Geophys. Res.*, *106*, 5437–5456, doi:10.1029/2000JD900574.

Cooper, O. R., et al. (2004), A case study of transpacific warm conveyor belt transport: Influence of merging airstreams on trace gas import to North America, *J. Geophys. Res.*, *109*, D23S08, doi:10.1029/2003JD003624.

de Gouw, J. A., et al. (2006), Volatile organic compounds composition of merged and aged forest fire plumes from Alaska and western Canada, *J. Geophys. Res.*, *111*, D10303, doi:10.1029/2005JD006175.

Derwent, R. G., D. S. Stevenson, W. J. Collins, and C. E. Johnson (2004), Intercontinental transport and the origins of the ozone observed at surface sites in Europe, *Atmos. Environ.*, *38*, 1891–1901.

Duncan, B. D., J. A. Logan, I. Bey, I. Megretskaia, R. M. Yantosca, P. C. Novelli, N. B. Jones, and C. P. Rinsland (2007), The global budget of CO, 1988–1997: Source estimates and validation with a global model, *J. Geophys. Res.*, *112*, D22301, doi:10.1029/2007JD008459.

Emmons, L. K., et al. (2006), Sensitivity of chemical budgets to meteorology in MOZART-4, *Eos Trans. AGU*, *87*(52), Fall Meet. Suppl., Abstract A51C-0094.

Fang, Y., C. Zhao, and C. Li (2005), Analysis of the distribution of carbon monoxide from MOPITT over East Asia in 2002, *Chin. J. Atmos. Sci.*, *29*(4), 407–416.

Fang, Y., A. Fiore, L. Horowitz, H. Levy, Y. Hu, and A. Russell (2008), Export of NO_y from the United States during summer 2004, *Eos Trans. AGU*, *89*(53), Fall Meet. Suppl., Abstract A21B–0134.

Fiore, A. M., L. W. Horowitz, E. J. Dlugokencky, and J. J. West (2006), Impact of meteorology and emissions on methane trends, 1990–2004, *Geophys. Res. Lett.*, *33*, L12809, doi:10.1029/2006GL026199.

Frost, G. J., et al. (2006), Effects of changing power plant NO_x emissions on ozone in the eastern United States: Proof of concept, *J. Geophys. Res.*, *111*, D12306, doi:10.1029/2005JD006354.

Fuelberg, H. E., M. Porter, C. M. Kiley, and D. Morse (2007), Meteorological conditions and anomalies during INTEX-NA, *J. Geophys. Res.*, *112*, D12S06, doi:10.1029/2006JD007734.

Griffin, R. J., J. Chen, K. Carmody, S. Vutukuru, and D. Dabdub (2007), Contribution of gas phase oxidation of volatile organic compounds to atmospheric carbon monoxide levels in two areas of the United States, *J. Geophys. Res.*, *112*, D10S17, doi:10.1029/2006JD007602.

Guerova, G., I. Bey, J-.L. Attie, and R. V. Martin (2006), Case studies of ozone transport between North America and Europe in summer 2000, *Atmos. Chem. Phys. Discuss.*, *5*, 6127–6184.

Holloway, T., A. Fiore, and M. G. Hastings (2003), Intercontinental transport of air pollution: Will emerging science lead to a new hemispheric treaty?, *Environ. Sci. Technol.*, *37*, 4535–4542, doi:10.1021/es034031g.

Horowitz, L. W., J. Liang, G. M. Gardner, and D. J. Jacob (1998), Export of reactive nitrogen from North America during summertime: Sensitivity to hydrocarbon chemistry, *J. Geophys. Res.*, *103*(D11), 13,451–13,476.

Horowitz, L. W., et al. (2003), A global simulation of tropospheric ozone and related tracers: Description and evaluation of MOZART, version 2, *J. Geophys. Res.*, *108*(D24), 4784, doi:10.1029/2002JD002853.

Horowitz, L. W., A. M. Fiore, G. P. Milly, R. C. Cohen, A. Perring, P. J. Wooldridge, P. G. Hess, L. K. Emmons, and J.-F. Lamarque (2007), Observational constraints on the chemistry of isoprene nitrates over the eastern United States, *J. Geophys. Res.*, *112*, D12S08, doi:10.1029/2006JD007747.

Hudman, R. C., et al. (2007), Surface and lightning sources of nitrogen oxides over the United States: Magnitudes, chemical evolution, and outflow, *J. Geophys. Res.*, *112*, D12S05, doi:10.1029/2006JD007912.

Hudman, R. C., L. T. Murray, D. J. Jacob, D. B. Millet, S. Turquety, S. Wu, D. R. Blake, A. H. Goldstein, J. Holloway, and G. W. Sachse (2008), Biogenic versus anthropogenic sources of CO in the United States, *Geophys. Res. Lett.*, *35*, L04801, doi:10.1029/2007GL032393.

Huntrieser, H., et al. (2005), Intercontinental air pollution transport from North America to Europe: Experimental evidence from airborne measurements and surface observations, *J. Geophys. Res.*, *110*, D01305, doi:10.1029/2004JD005045.

Kiley, C. M., and H. E. Fuelberg (2006a), An examination of summertime cyclone transport processes during Intercontinental Chemical Transport Experiment (INTEX-A), *J. Geophys. Res.*, *111*, D24S06, doi:10.1029/2006JD007115.

Kiley, C. M., and H. E. Fuelberg (2006b), An examination of summertime transport processes during INTEX-A using meteorological analyses and synthetic MOPITT carbon monoxide retrievals, Ph.D. dissertation, 94 pp., Fla. State Univ., Tallahassee. (Available at http://etd.lib.fsu.edu/theses/available/etd-10302006-221246/)

Lambert, S. J., and J. C. Fyfe (2006), Changes in winter cyclone frequencies and strengths simulated in enhanced greenhouse warming experiments: Results from the models participating in the IPCC diagnostic exercise, *Clim. Dyn.*, *26*, 713–728, doi:10.1007/s00382-006-0110-3.

Li, Q., et al. (2002), Transatlantic transport of pollution and its effects on surface ozone in Europe and North America, *J. Geophys. Res.*, *107*(D13), 4166, doi:10.1029/2001JD001422.

Li, Q., D. Jacob, R. Park, Y. Wang, C. Heald, R. Hudman, R. Yantosca, R. Martin, and M. Evans (2005), North American pollution outflow and the trapping of convectively lifted pollution by upper-level anticyclone, *J. Geophys. Res.*, *110*, D10301, doi:10.1029/2004JD005039.

Liang, J., L. W. Horowitz, D. J. Jacob, Y. Wang, A. M. Fiore, J. A. Logan, G. M. Gardner, and J. W. Munger (1998), Seasonal budgets of reactive nitrogen species and ozone over the United States, and export fluxes to the global atmosphere, *J. Geophys. Res.*, *103*, 13,435–13,450.

McCabe, G. J., M. P. Clark, and M. C. Serreze (2001), Trends in Northern Hemisphere surface cyclone frequency and intensity, *J. Clim.*, *14*, 2763–2768, doi:10.1175/1520-0442(2001)014<2763:TINHSC>2.0.CO;2.

Merrill, J. T., and J. L. Moody (1996), Synoptic meteorology and transport during the North Atlantic Regional Experiment (NARE) intensive: Overview, *J. Geophys. Res.*, *101*, 28,903–28,921.

Mickley, L. J., D. J. Jacob, B. D. Field, and D. Rind (2004), Effects of future climate change on regional air pollution episodes in the United States, *Geophys. Res. Lett.*, *31*, L24103, doi:10.1029/2004GL021216.

Nichols, N., G. Gruza, J. Jouzel, T. Karl, L. Ogallo, and D. Parker (2001), Observed climate variability and change, in *Climate Change 2001: The Scientific Basis. Contribution of Working Group I to the Third Assessment Report of the Intergovernmental Panel on Climate Change*, edited by J. T. Houghton et al., pp. 99–182, Cambridge Univ. Press, Cambridge, U. K.

Olivier, J. G. J., and J. J. M. Berdowski (2001), Global emissions sources and sinks, in *The Climate System*, edited by J. Berdowski, R. Guicherit, and B. J. Heij, pp. 33–78, A.A. Balkema, Lisse, Netherlands.

Olivier, J., J. Peters, C. Granier, G. Pétron, J. F. Müller, and S. Wallens (2003), Present and future surface emissions of atmospheric compounds, *POET Rep. 2*, Neth. Environ. Assess. Agency, Bilthoven, Netherlands.

Ott, L. E., K. E. Pickering, G. L. Stenchikov, H. Huntrieser, and U. Schumann (2007), Effects of lightning NO_x production during the 21 July European Lightning Nitrogen Oxides Project storm studied with a three-dimensional cloud-scale chemical transport model, *J. Geophys. Res.*, *112*, D05307, doi:10.1029/2006JD007365.

Owen, R. C., O. R. Cooper, A. Stohl, and R. E. Honrath (2006), An analysis of the mechanisms of the North American pollutant transport to the central North Atlantic lower free troposphere, *J. Geophys. Res.*, *111*, D23S58, doi:10.1029/2006JD007062.

Pickering, K. E., et al. (2006), Using results from cloud-resolving models to improve lightning NO_x parameterizations for global chemical transport and climate models, *Eos Trans. AGU*, *87*(36), Jt. Assem. Suppl., Abstract A52B-05.

Pierce, R. B., et al. (2007), Chemical data assimilation estimates of continental U. S. ozone and nitrogen budgets during the Intercontinental Chemical Transport Experiment–North America, *J. Geophys. Res.*, *112*, D12S21, doi:10.1029/2006JD007722.

Singh, H. B., W. Brune, J. Crawford, and D. Jacob (2006), Overview of the summer 2004 Intercontinental Chemical Transport Experiment–North America (INTEX-NA), *J. Geophys. Res.*, *111*, D24S01, doi:10.1029/2006JD007905.

Staudt, A. C., D. J. Jacob, J. A. Logan, D. Bachiochi, T. N. Krishnamurti, and G. W. Sachse (2001), Continental sources, transoceanic transport, and interhemispheric exchange of carbon monoxide over the Pacific, *J. Geophys. Res.*, *106*, 32,571–32,589, doi:10.1029/2001JD900078.

Stohl, A. (2001), A 1-year Lagrangian "climatology" of airstreams in the Northern Hemisphere troposphere and lowermost stratosphere, *J. Geophys. Res.*, *106*(D7), 7263–7279.

Stohl, A., and T. Trickl (1999), A textbook example of long-range transport: Simultaneous observation of ozone maxima of stratospheric and North American origin in the free troposphere over Europe, *J. Geophys. Res.*, *104*, 30,445–30,462, doi:10.1029/1999JD900803.

Stohl, A., et al. (2003), Rapid intercontinental air pollution transport associated with a meteorological bomb, *Atmos. Chem. Phys.*, *3*, 969–985.

Tie, X., S. Madronich, S. Walters, D. P. Edwards, P. Ginoux, N. Mahowald, R. Zhang, C. Lou, and G. Brasseur (2005), Assessment of the global impact of aerosols on tropospheric oxidants, *J. Geophys. Res.*, *110*, D03204, doi:10.1029/2004JD005359.

Trickl, T., O. R. Cooper, H. Eisele, P. James, R. Mücke, and A. Stohl (2003), Intercontinental transport and its influence on the ozone concentrations over central Europe: Three case studies, *J. Geophys. Res.*, *108*(D12), 8530, doi:10.1029/2002JD002735.

Turquety, S., et al. (2007), Inventory of boreal fire emissions for North America in 2004: Importance of peat burning and pyroconvective injection, *J. Geophys. Res.*, *112*, D12S03, doi:10.1029/2006JD007281.

Vukovich, F. M. (1995), Regional-scale boundary layer ozone variations in the eastern United States and their association with meteorological variations, *Atmos. Environ.*, *29*(17), 2259–2273, doi:10.1016/1352-2310(95)00146-P.

Wild, O., and H. Akimoto (2001), Intercontinental transport of ozone and its precursors in a three-dimensional global CTM, *J. Geophys. Res.*, *106*, 27,729–27,744, doi:10.1029/2000JD000123.

Wild, O., K. S. Law, D. S. McKenna, B. J. Bandy, S. A. Penkett, and J. A. Pyle (1996), Photochemical trajectory modeling studies of the North Atlantic region during August 1993, *J. Geophys. Res.*, *101*(D22), 29,269–29,288, doi:10.1029/96JD00837.

Y. Fang, A. Gnanadesikan, and L. W. Horowitz, Atmospheric and Oceanic Sciences Program, Princeton University, Princeton, NJ 08540, USA. (yfang@princeton.edu)

A. M. Fiore and H. Levy II, Geophysical Fluid Dynamics Laboratory, Princeton, NJ 08540, USA.

Y. Hu and A. G. Russell, School of Civil and Environmental Engineering, Georgia Institute of Technology, Atlanta, GA 30332, USA.